CHAPTER 4

INFINITE SPEED BEHAVIOR OF TWO-TEMPERATURE GREEN LINDSAY THERMOELASTICITY THEORY UNDER TEMPERATURE DEPENDENT THERMAL CONDUCTIVITY[1]

4.1 Introduction

It has been realized that the thermoelastic parameters are assumed to be constant in general but at very high temperature these parameters remain no longer constants for thermoelastic materials. It has been reported by Noda (1986) with practical results that thermal conductivity of the materials decrease linearly with temperature. Thermoelastic materials at high temperature provides much different practical and theoretical results from the expectations. Therefore, it is quite necessary to consider the dependency of these parameters on temperature in the analysis of the behavior of materials in particular, when it is kept at very high temperature. In recent years, some work have been carried out with generalized theory of thermoelasticity by taking into account the dependency of thermoelastic parameters on temperature. Suhara (1918) solved a thermoelastic model by considering the shear modulus depending on temperature and discussed the effect in details. Youssef and Abbas (2007) discussed the results by

[1]The content of this chapter is ***communicated*** **to an** ***International Journal*****, 2018**.

solving a thermoelastic problem for an unbounded medium with a spherical cavity by assuming that thermal conductivity and modulus of elasticity depend on temperature. A characteristic feature has been discussed for a two-dimensional thermoelastic problem with temperature dependent elastic moduli by Othman (2002; 2003; 2013; 2015). Zenkour and Abbas (2014) discussed the effects of temperature dependent properties of the materials assuming the density and other thermoelastic properties depending on temperature.

The present chapter of the thesis is concerned with the analysis of the effects of temperature dependent thermal conductivity on thermoelastic interactions inside a medium with a spherical cavity under two-temperature generalized thermoelastic theory that involves two thermal relaxation parameters. The thermal conductivity of the material is assumed to vary with temperature linearly. Initially, the temperature at the boundary of the spherical cavity is assumed to be subjected to a thermal shock and it is assumed that there is no stress on the surface of the cavity. We solve the problem by using Kirchhoff transformation along with Laplace transform technique. Various graphs are plotted to display the distributions of different field variables like, conductive temperature, thermodynamic temperature, displacement and two non-zero components of stress. An attempt is also made to compare the results in the present context with the corresponding results predicted by other thermoelasticity theories. A detailed analysis of our results due to temperature dependent material properties and the effects of employing two-temperature model is presented. We highlight some important features of the present two-temperature model in the context of temperature dependent thermal conductivity.

4.2 Problem Formulation

We consider an isotropic elastic medium with temperature dependent material properties. We write the basic governing equations under four models namely Lord-Shulman (LS) model (1967), Green-Lindsay (GL)(1972) model, two-temperature LS model (TLS model: Youssef (2006b)) and two-temperature GL model (TGL model: Youssef (2006b)) in unified way as follows:

The equation of motion:

$$\sigma_{ij,j} = \rho \ddot{u}_i \tag{4.1}$$

The equation of heat conduction:

$$\left(K\phi_{,i}\right)_{,i} = \left(1 + \xi\tau_0 \frac{\partial}{\partial t}\right)\left[\rho c_E \frac{\partial \theta}{\partial t} + T_0 \gamma \frac{\partial e}{\partial t}\right] \tag{4.2}$$

where

$$\phi - \theta = \alpha \phi_{,ii} \tag{4.3}$$

The equation of stress-strain-temperature relation:

$$\sigma_{ij} = 2\mu e_{ij} + \lambda e_{kk}\delta_{ij} - \gamma\left(\theta + \tau_1 \frac{\partial \theta}{\partial t}\right)\delta_{ij} \tag{4.4}$$

Strain-displacement relation:

$$e_{ij} = \frac{1}{2}\left(u_{i,j} + u_{j,i}\right) \tag{4.5}$$

Using equations (4.1) and (4.4), we find

$$\mu u_{i,jj} + (\lambda + \mu) u_{j,ji} - \gamma \left(\theta + \tau_1 \frac{\partial \theta}{\partial t} \right)_i = \rho \ddot{u}_i \tag{4.6}$$

Here, α is the two-temperature parameter which is the characteristic of the present model.

The above set of equations (4.1)-(4.6) can be reduced to the corresponding equations of TGL, GL, TLS and LS models by providing the particular values to the parameters α, τ_0, τ_1 and ξ as follows:

- **TGL model:** $\alpha \neq 0$, $\tau_0 \neq 0$, $\tau_1 \neq 0$ and $\xi = 0$
- **GL model:** $\alpha = 0$, $\tau_0 \neq 0$, $\tau_1 \neq 0$ and $\xi = 0$
- **TLS model:** $\alpha \neq 0$, $\tau_0 \neq 0$, $\tau_1 = 0$ and $\xi = 1$
- **LS model:** $\alpha = 0$, $\tau_0 \neq 0$, $\tau_1 = 0$ and $\xi = 1$

We suppose that the thermal conductivity, K varies with temperature and assume that it is varying as

$$K(\phi) = K_0(1 + K_1\phi) \tag{4.7}$$

where K_0 is the thermal conductivity at reference temperature T_0. K_1 is a constant, which is zero at reference temperature, T_0.

We consider an unbounded thermoelastic medium with a spherical cavity of radius a, initially at uniform temperature T_0. In the case when we consider the center of the cavity at the origin and spherical symmetry by introducing spherical polar coordinates (r, ϑ, φ), equations (4.2)-(4.4) and (4.6) reduce to the following forms:

$$(\lambda + 2\mu)\frac{\partial e}{\partial r} - \gamma\left(1 + \tau_1\frac{\partial}{\partial t}\right)\frac{\partial \theta}{\partial r} = \rho\frac{\partial^2 u}{\partial t^2} \tag{4.8}$$

$$\left[K\nabla^2\phi + \frac{\partial K}{\partial \phi}\left(\frac{\partial \phi}{\partial r}\right)^2\right] = \left(1 + \xi\tau_0\frac{\partial}{\partial t}\right)\left(\rho c_E\frac{\partial \theta}{\partial t} + \gamma T_0\frac{\partial e}{\partial t}\right) \tag{4.9}$$

$$\sigma_{rr} = 2\mu\frac{\partial u}{\partial r} + \lambda e - \gamma\left(\theta + \tau_1\frac{\partial \theta}{\partial t}\right) \tag{4.10}$$

$$\sigma_{\varphi\varphi} = \sigma_{\vartheta\vartheta} = 2\mu\frac{u}{r} + \lambda e - \gamma\left(\theta + \tau_1\frac{\partial \theta}{\partial t}\right) \tag{4.11}$$

$$\phi - \theta = \alpha\nabla^2\phi \tag{4.12}$$

where u is the single non-zero component of displacement. σ_{rr}, $\sigma_{\varphi\varphi}$ and $\sigma_{\vartheta\vartheta}$ are non-zero stress components, $e = \frac{\partial u}{\partial r} + \frac{2}{r}u$ and $\nabla^2 = \frac{\partial^2}{\partial r^2} + \frac{2}{r}\frac{\partial}{\partial r}$.

In view of equations (4.7,4.12), we find that equation (4.9) is non-linear, and therefore to tackle the non-linearity we consider a new function Φ expressing the temperature with Kirchhoff transformation as

$$\Phi = \frac{1}{K_0}\int_0^{\phi} K(p)dp = \phi + \frac{1}{2}K_1\phi^2 \tag{4.13}$$

Hence, by using equations (4.7) and (4.13), we have

$$K_0\frac{\partial \Phi}{\partial r} = K\frac{\partial \phi}{\partial r} \; and \; K_0\frac{\partial^2 \Phi}{\partial r^2} = K\frac{\partial^2 \phi}{\partial r^2} + \frac{\partial K}{\partial \phi}\left(\frac{\partial \phi}{\partial r}\right)^2$$

Therefore, we get

$$\left[K\nabla^2\phi + \frac{\partial K}{\partial \phi}\left(\frac{\partial \phi}{\partial r}\right)^2\right] = K_0\nabla^2\Phi \tag{4.14}$$

Employing equation (4.14) into equation (4.9), we have

$$K_0\nabla^2\Phi = \left(1 + \xi\tau_0\frac{\partial}{\partial t}\right)\left(\rho c_E\frac{\partial \theta}{\partial t} + \gamma T_0\frac{\partial e}{\partial t}\right) \tag{4.15}$$

Now, for convenience we use the following symbols and notations in order to make equations (4.8), (4.10)-(4.12) and (4.15) dimensionless:

$(r', u') = c_0\eta\,(r, u)$, $\left(t', \tau_0^{'}, \tau_1^{'}\right) = c_0^2\eta\,(t, \tau_0, \tau_1)$, $\left(\theta^{'}, \phi^{'}, \Phi'\right) = \frac{1}{T_0}\,(\theta - T_0, \phi - T_0, \Phi - T_0)$,

$e' = e,\ \sigma_{ij}' = \frac{\sigma_{ij}}{(\lambda_0+2\mu_0)},\ c_0^2 = \frac{(\lambda+2\mu)}{\rho},\ a_1 = \frac{\gamma T_0}{(\lambda+2\mu)},\ a_2 = \frac{\gamma}{K_0\eta},\ a_3 = \alpha c_0^2\eta^2,$
$\lambda_1 = \frac{\lambda}{(\lambda+2\mu)}$.

where $\eta = \frac{\rho c_E}{K_0}$.

Therefore, equations (4.8), (4.10)-(4.12) and (4.15) change to their dimensionless forms, after dropping the primes for clarity, as follows:

$$\frac{\partial e}{\partial r} - a_1\left(1 + \tau_1\frac{\partial}{\partial t}\right)\frac{\partial \theta}{\partial r} = \frac{\partial^2 u}{\partial t^2} \tag{4.16}$$

$$\nabla^2\dot{\Phi} = \left(1 + \xi\tau_0\frac{\partial}{\partial t}\right)\left(\frac{\partial \theta}{\partial t} + a_2\frac{\partial e}{\partial t}\right) \tag{4.17}$$

$$\sigma_{rr} = (1 - \lambda_1)\frac{\partial u}{\partial r} + \lambda_1 e - a_1\left(\theta + \tau_1\frac{\partial \theta}{\partial r}\right) \tag{4.18}$$

$$\sigma_{\varphi\varphi} = \sigma_{\vartheta\vartheta} = (1 - \lambda_1)\frac{u}{r} + \lambda_1 e - a_1\left(\theta + \tau_1\frac{\partial \theta}{\partial r}\right) \tag{4.19}$$

$$\phi - \theta = a_3 \nabla^2 \phi \tag{4.20}$$

4.3 Solution of the Problem

We apply Laplace transform to the equations (4.16)-(4.20) with homogeneous initial conditions and we obtain

$$\frac{\partial \bar{e}}{\partial r} - b_0(s) \frac{\partial \bar{\theta}}{\partial r} = s^2 \bar{u} \tag{4.21}$$

$$\nabla^2 \bar{\Phi} = b_1(s) \left(\bar{\theta} + a_2 \bar{e} \right) \tag{4.22}$$

$$\bar{\sigma}_{rr} = (1 - \lambda_1) \frac{\partial \bar{u}}{\partial r} + \lambda_1 \bar{e} - b_0(s) \bar{\theta} \tag{4.23}$$

$$\bar{\sigma}_{\varphi\varphi} = \bar{\sigma}_{\nu\nu} = (1 - \lambda_1) \frac{\bar{u}}{r} + \lambda_1 \bar{e} - b_0(s) \bar{\theta} \tag{4.24}$$

$$\bar{\phi} - \bar{\theta} = a_3 \nabla^2 \bar{\phi} \tag{4.25}$$

where $b_0(s) = a_1 (1 + \tau_1 s)$ and $b_1(s) = s (1 + \xi \tau_0 s)$.

Now taking divergence of equation (4.21), we get

$$\nabla^2 \bar{e} - b_0(s) \nabla^2 \bar{\theta} = s^2 \bar{e} \tag{4.26}$$

From equations (4.22) and (4.25) $\left(\text{using the fact} \left| \frac{\phi}{T_0} \right| << 1 \right)$, we find

$$b_2(s)\nabla^2\bar{\Phi} = b_1(s)\bar{\Phi} + a_2 b_1(s)\bar{e} \tag{4.27}$$

where $b_2(s) = 1 + a_3 b_1(s)$.

Similarly, by using equation (4.25) into equation (4.26), we get the following equation:

$$a_3 b_0(s)\nabla^4\bar{\Phi} - b_0(s)\nabla^2\bar{\Phi} + \nabla^2\bar{e} = s^2\bar{e} \tag{4.28}$$

Applying equation (4.27) into (4.28), we find

$$m_0(s)\nabla^4\bar{\Phi} - m_1(s)\nabla^2\bar{\Phi} + m_2(s)\bar{\Phi} = 0 \tag{4.29}$$

where $m_0(s) = a_2 a_3 b_0(s) b_1(s) + b_2(s)$, $m_1(s) = a_2 b_0(s) b_1(s) + b_1(s) + s^2 b_2(s)$, $m_2(s) = s^2 b_1(s)$.

Further, using equation (4.27) into (4.28) repeatedly, we find

$$p_0(s)\bar{\Phi} + p_1(s)\nabla^2\bar{e} + p_2(s)\bar{e} = 0 \tag{4.30}$$

where $p_0(s) = b_0(s)b_1(s)\left[a_3 b_1(s) - b_2(s)\right]$, $p_1(s) = b_2(s)\left[a_2 a_3 b_0(s) b_1(s) + b_2(s)\right]$, $p_2(s) = a_2 a_3 b_0(s) b_1^2(s) - a_2 b_0(s) b_1(s) b_2(s) - s b_2^2(s)$.

Applying equation (4.30) into equation (4.27), we have

$$n_0(s)\nabla^4\bar{e} - n_1(s)\nabla^2\bar{e} + n_2(s)\bar{e} = 0 \tag{4.31}$$

where $n_0(s) = b_2(s)p_1(s)$, $n_1(s) = p_1(s)b_1(s) - p_2(s)b_2(s)$, $n_2(s) = b_1(s)\left[a_2 p_0(s) - p_2(s)\right]$.

The equations (4.29) and (4.31) are in the form of modified spherical

Bessel differential equations, hence its bounded solution can be obtained in the forms

$$\bar{\Phi}(r,s) = \frac{1}{\sqrt{r}} \sum_{j=1}^{2} A_j K_{1/2}(c_j r) \tag{4.32}$$

$$\bar{e}(r,s) = \frac{1}{\sqrt{r}} \sum_{j=1}^{2} B_j K_{1/2}(d_j r) \tag{4.33}$$

where, A_j and B_j are arbitrary constants, $K_\alpha(r)$ is the representation of modified Bessel functions of order α of second kinds, respectively and $\pm c_j$ and $\pm d_j$ $(j = 1, 2)$ are roots of the equations

$m_0(s)x^4 - m_1(s)x^2 + m_2(s) = 0$ and $n_0(s)x^4 - n_1(s)x^2 + n_2(s) = 0$, respectively.

Applying equations (4.32) and (4.33) into (4.27), we have

$$K_{1/2}(d_j r)B_j = b_3^{(j)}(s)K_{1/2}(c_j r)A_j, \quad j = 1, 2 \tag{4.34}$$

where $b_3^{(j)}(s) = \frac{b_2(s)c_j^2 - b_1(s)}{a_2 b_1(s)}$,

Using equations (4.25), (4.32) and (4.33) into (4.21), we have

$$\bar{u}(r,s) = \frac{1}{\sqrt{r}} \left[-\sum_{j=1}^{2} \frac{d_j}{s^2} K_{3/2}(d_j r)B_j + \sum_{j=1}^{2} b_4^{(j)}(s)K_{3/2}(c_j r)A_j \right] \tag{4.35}$$

where $b_4^{(j)}(s) = \frac{b_0(s)c_j\left[1 - a_3 c_j^2\right]}{s^2}$

From equations (4.23) and (4.25), we get

$$\bar{\sigma}_{rr} = \frac{1}{\sqrt{r}} \sum_{j=1}^{2} \left[\frac{(1-\lambda_1)\, d_j^2}{s^2} + \lambda_1 \right] K_{1/2}(d_j r) B_j + \frac{1}{r^{3/2}} \sum_{j=1}^{2} \frac{2 d_j\,(1-\lambda_1)}{s^2} K_{3/2}(d_j r) B_j$$
$$- \frac{1}{\sqrt{r}} \sum_{j=1}^{2} \left[(1-\lambda_1)\, c_j b_4^{(j)}(s) + \lambda_1 b_0(s) + a_3 c_j^2 b_0(s) \right] K_{1/2}(c_j r) A_j$$
$$- \frac{1}{r^{3/2}} \sum_{j=1}^{2} 2\,(1-\lambda_1)\, b_4^{(j)}(s) K_{3/2}(c_j r) A_j \tag{4.36}$$

Similarly, we find the solutions for the stress components from equations (4.24) and (4.25) as

$$\bar{\sigma}_{\varphi\varphi} = \bar{\sigma}_{\vartheta\vartheta} = \frac{1}{\sqrt{r}} \sum_{j=1}^{2} \lambda_1 K_{1/2}(d_j r) B_j - \frac{1}{r^{3/2}} \sum_{j=1}^{2} \frac{d_j\,(1-\lambda_1)}{s^2} K_{3/2}(d_j r) B_j$$
$$- \frac{1}{\sqrt{r}} \sum_{j=1}^{2} b_0(s) \left(1 - a_3 c_j^2\right) K_{1/2}(c_j r) A_j + \frac{1}{r^{3/2}} \sum_{j=1}^{2} (1-\lambda_1)\, b_4^{(j)}(s) K_{3/2}(c_j r) A_j \tag{4.37}$$

4.3.1 Boundary Conditions

We consider the boundary $r = a$ of the spherical cavity is traction free and is subjected to a unit step increase in temperature. Therefore, the boundary conditions in the dimension-less forms can be written as:

$$\phi(r,t) = \phi_0^* H(t) \text{ and } \quad \sigma_{rr}(r,t) = 0 \text{ at } r = a \tag{4.38}$$

where ϕ_0^* is a constant temperature and $H(t)$ is the Heaviside unit-step function.

Therefore, using equations (4.13) and applying Laplace transform to the boundary conditions given by(4.38), we find that

$$\bar{\Phi}(a,s) = \frac{\phi_0^*}{s}\left(1 + \frac{1}{2}K_1\phi_0^*\right), \quad \bar{\sigma}_{rr}(a,s) = 0. \tag{4.39}$$

From equations (4.32), (4.34) and (4.39), we obtain a linear system of two equations as given by

$$X_1A_1 + X_2A_2 = \frac{\phi_0^*}{s}\left(1 + \frac{1}{2}K_1\phi_0^*\right) \tag{4.40}$$

$$Y_1A_1 + Y_2A_2 = 0 \tag{4.41}$$

where

$$X_j = \frac{1}{\sqrt{a}}K_{1/2}(c_ja), \quad j = 1,2.$$

$$Y_j = \frac{1}{\sqrt{a}}\left[\frac{(1-\lambda_1)\,d_j^2}{s^2} + \lambda_1\right] b_3^{(j)} K_{1/2}(c_ja) + \frac{2d_j\,(1-\lambda_1)\,b_3^{(j)}}{s^2a^{3/2}}\frac{K_{1/2}(c_ja)K_{3/2}(d_ja)}{K_{1/2}(d_ja)}$$
$$- \frac{1}{\sqrt{a}}\left[(1-\lambda_1)\,c_jb_4^{(j)}(s) + \lambda_1b_0(s) + a_3c_j^2b_0(s)\right]K_{1/2}(c_ja)$$
$$- \frac{2\,(1-\lambda_1)\,b_4^{(j)}(s)}{a^{3/2}}K_{3/2}(c_ja)$$

here, j=1,2.

After solving the equations (4.40)-(4.41), we can find the unknowns A_j $(j = 1,2)$ and hence the constants $B_j,\ j = 1,2$, from equation (4.34). This completes the solution of the present problem in Laplace transform domain as displacement, radial stress and shear stress can be obtained with the help of equations (4.35)-(4.37), respectively and conductive temperature, $\bar{\phi}$ can be obtained by combining equation (4.32) with (4.13) . We can obtain the solution for thermodynamic temperature, θ in the Laplace transform domain by using equations (4.22).

4.4 Numerical Results and Discussion

The solution in the physical space-time domain can be obtained by taking the inverse Laplace transform of the obtained results. But as the expressions of $\bar{\theta}$, $\bar{u}$, $\bar{\sigma}_{rr}$ and $\bar{\sigma}_{\varphi\varphi}$ involve complicated expressions of Laplace transform parameter s, therefore it is a formidable task to find the solution in space-time domain analytically. However, we obtain the Laplace inversion for physical variables like, conductive temperature ϕ , the thermodynamic temperature $\bar{\theta}$, displacement $\bar{u}$, radial stress $\bar{\sigma}_{rr}$ and shear stress $\bar{\sigma}_{\varphi\varphi}$ taking the help of MATLAB software and by employing Stehfest (1970) (see Appendix. A-1) numerical method of Laplace inversion. According to this method, if $\overline{f}(s)$ is the Laplace inverse of the function $f(t)$, then

$$f(t) = \frac{ln(2)}{2} \sum_{k=1}^{N} V_k \overline{f} \left(k \frac{ln(2)}{t} \right) \tag{4.42}$$

where N is the suitable positive integer and V_k is given by

$$V_k = (-1)^{(k+N/2)} \sum_{j=[(k+1)/2]}^{\min(k,N/2)} \frac{j^{\frac{N}{2}} \, (2j)!}{\left(\frac{N}{2} - j\right)! \; j! \;\; (j-1)! \, (k-j)! \, (2j-k)!} \tag{4.43}$$

We consider copper material and the physical data as follows (Sherief and Salah (2005)):

$\lambda = 7.76 \times 10^{10} Nm^{-2}$, $\mu = 3.86 \times 10^{10} Nm^{-2}$, $\alpha_t = 1.78 \times 10^{-5} K^{-1}$, $\eta = 8886.73 sm^{-2}$, $c_E = 383.1 JKg^{-1}K^{-1}$, $\rho = 8954 Kg\ m^{-3}$, $T_0 = 293K$.

We assume the following dimension-less values of the constants:

$\alpha = 0.071301$, $\tau_0 = 0.01$, $\tau_1 = 0.02$, $\phi_1^* = 1$.

We make an attempt to discuss the results under all four models and hence we obtain the numerical results of physical variables, u, ϕ, σ_{rr}, $\sigma_{\varphi\varphi}$ and θ at different times. We show the results by different graphs. Figs.4.1(a), 4.2(a), 4.3(a), 4.4(a) and 4.5(a) show the variations of displacement, conductive and thermodynamic temperatures, radial stress and hoop stress, respectively under two-temperature Green-Lindsay thermoelasticity theory for different values of parameter, K_1 and at different non-dimensional times, $t = 0.30$, $t = 0.35$, $t = 0.40$. Figs.4.1(b), 4.2(b), 4.3(b), 4.4(b) and 4.5(b) depict the variations of all the field variables for TGL.,GL, TLS and LS thermoelasticity models for $K_1 = -0.5$ and at time $t = 0.3$. We find the following observations for different physical fields:

4.4.1 Displacement, u

Fig. 4.1(a) shows the effects of parameter K_1 on displacement for TGL model and we note that the influence region is dominant near the boundary of the spherical cavity and it is insignificant when we move away from boundary of the cavity. The effect of the temperature dependent effect parameter, $K_1$and time, t on displacement, is significant. It is observed that at any time the displacement increases as the value of K_1 goes to higher negative values. It is further observed that displacement is inversely proportional to the time, t for a fixed value of K_1, i.e. u decreases with

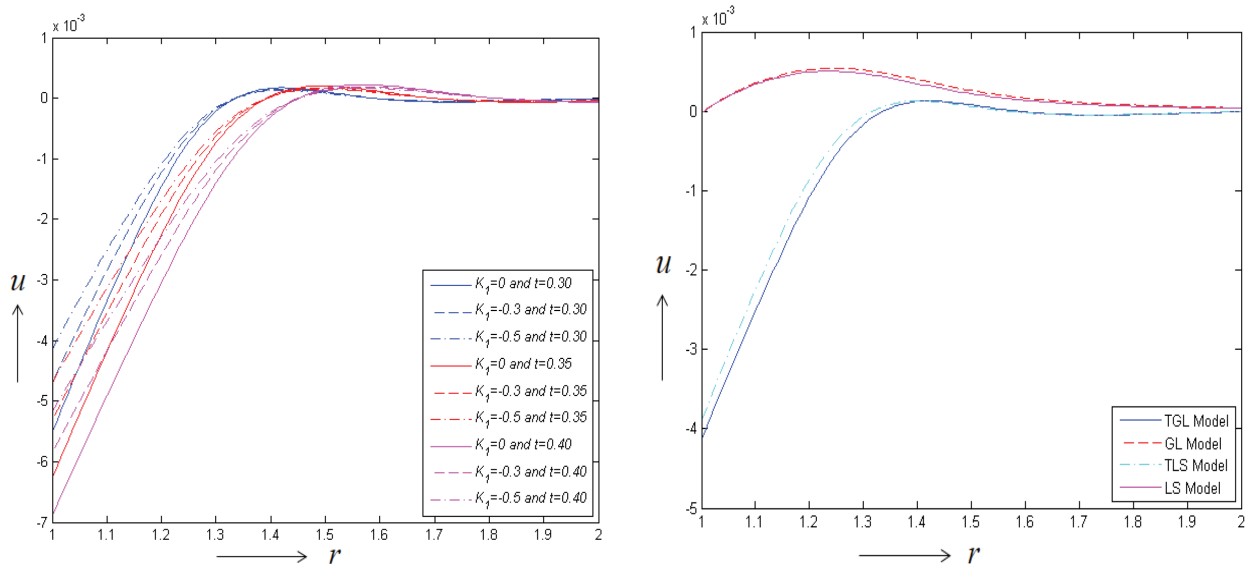

($\boldsymbol{a}$) ($\boldsymbol{b}$)

Figure 4.1: **($\boldsymbol{a}$).**Variation of u vs. r under TGL model for different values of t and K_1, **($\boldsymbol{b}$).**Variation of u vs. r for $K_1 = -0.5$ and $t = 0.3$ under different models

increase in time, t.

Fig. 4.1(b) shows that there is no prominent difference in displacement for GL and LS or TGL and TLS thermoelasticity theories. However, the difference is notable under a two-temperature thermoelasticity theory and without a two-temperature thermoelasticity theory. Displacement is zero at the boundary of the cavity for GL and LS theories while it is not same for two-temperature theories. It is also clear from the figure that displacement is positive for GL and LS theories while it is negative under TGL and TLS theories.

4.4.2 Conductive temperature, ϕ

Figs. 4.2(a) and 4.2(b) display the variation of conductive temperature, ϕ. It is indicated from Fig. 4.2(a) that the distribution of ϕ is in agreement with the given boundary condition. It further shows that for TGL thermoe-

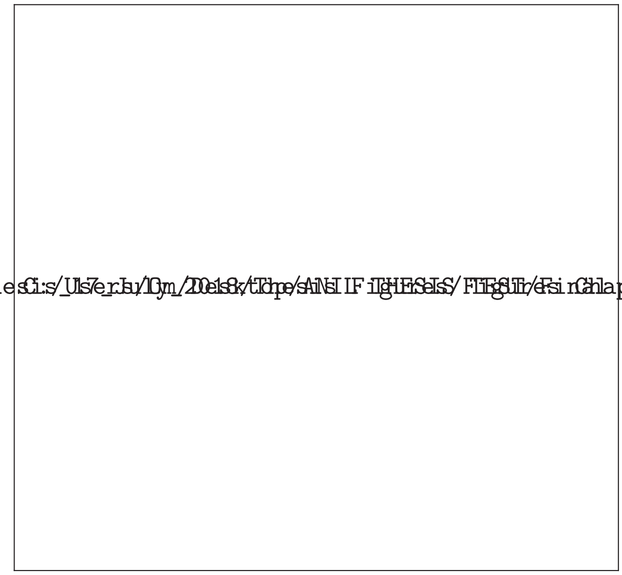

(*a*) **(b)**

Figure 4.2: **(*a*).**Variation of ϕ vs. r under TGL model for different values of t and K_1, **(*b*).**Variation of ϕ vs. r for $K_1 = -0.5$ and $t = 0.3$ under different modes

lasticity theory, the effect of temperature dependent material parameter, K_1 is much prominent at any time.

Similar to displacement, Fig.4.2(b) shows that the variation in ϕ is not prominent between TGL and TLS or between GL and LS theories while the variation becomes prominent between a two-temperature theory and without a two-temperature theory. Further, it is observed that ϕ tends to 0 as $r \to \infty$ but convergence speed is much slow for two-temperature theories. Region of influence is much larger in case of two-temperature theory as compared to generalized thermoelasticity theory.

4.4.3 Thermodynamic temperature, θ

We can see the variation of thermodynamic temperature, θ for TGL model for different values of parameter K_1 and time, t from Fig. 4.3(a). It is observed that θ is largely affected by temperature dependent parameter

C:/Users/Om/Desktop/ANIL THESIS TEST/Final The[illegible]

(***a***) (***b***)

Figure 4.3: (***a***)**.**Variation of θ vs. r under TGL model for different values of t and K_1, (***b***)**.**Variation of θ vs. r for $K_1 = -0.5$ and $t = 0.3$ under different models

K_1 and time.

However, a similar variation in thermodynamic temperature, θ is observed for a particular value of K_1 . The thermodynamic temperature, θ decreases for higher negative values of parameter, K_1. However, θ is affected negligibly with the increase of time for a fixed value of parameter, K_1 under TGL model.

Fig. 4.3(b) shows the variation of thermodynamic temperature, θ under four different models for a fixed value of parameter, K_1 at a fixed time. Here, it is depicted that, like the case of conductive temperature, there is no prominent difference in variation of θ for TGL and TLS models or between GL and LS models, but the difference in variation of θ is significant for a two-temperature model and without a two-temperature model. The thermodynamic temperature, θ converges to zero for LS and GL models very fast. However, we note that under TLS oand TGL models, it tends

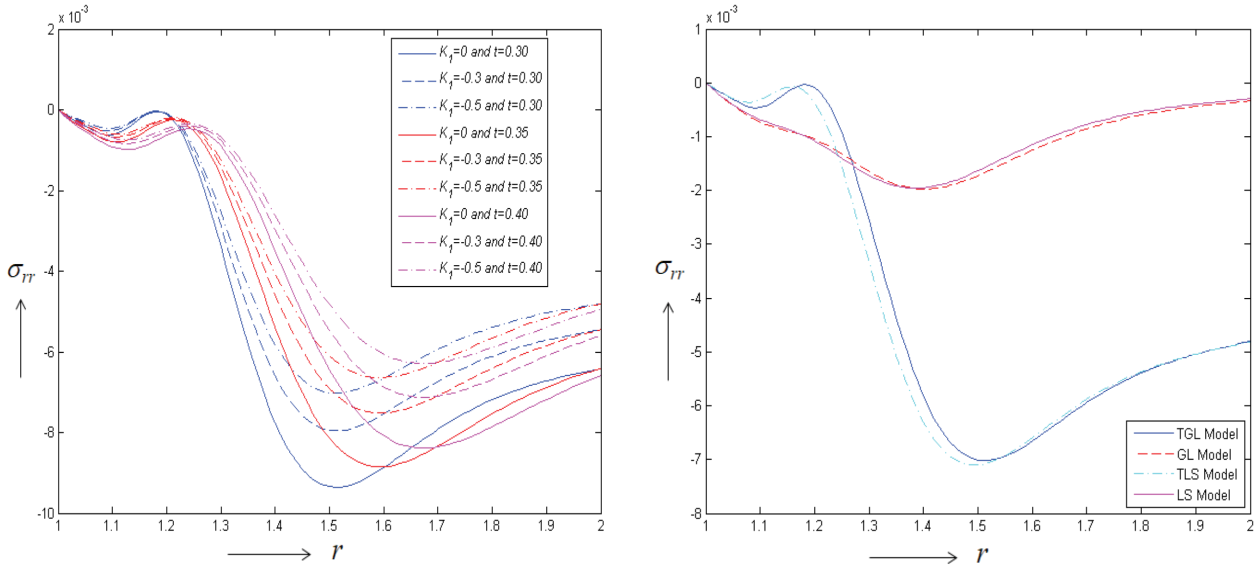

($\boldsymbol{a}$) ($\boldsymbol{b}$)

Figure 4.4: **($\boldsymbol{a}$).**Variation of σ_{rr} vs. r under TGL model for different values of t and K_1, **($\boldsymbol{b}$).**Variation of σ_{rr} vs. r for $K_1 = -0.5$ and $t = 0.3$ under different models

to zero as radial distance, $r \to \infty$ implying that the region of influence for TGL and TLS models is very large as compared to the cases of LS and GL models.

4.4.4 Stresses, σ_{rr} and $\sigma_{\varphi\varphi}$

The variation of radial stress, σ_{rr} is displayed in Figs. 4.4(a) and 4.4(b). Both of these figures reveal that the radial stress is in agreement with provided boundary condition. It is compressive in nature and has two clear minima points. It is evident from Fig. 4.4(a) that with respect to TGL model, the variation in radial stress is prominent corresponding to both time, t and temperature dependent effect parameter, K_1. Furthermore σ_{rr} increases if t increases or the parameter, K_1 gets higher negative values. Fig. 4.4(b) shows that the variation in σ_{rr} is prominent only with respect to a two-temperature theory and without a two-temperature theory as in

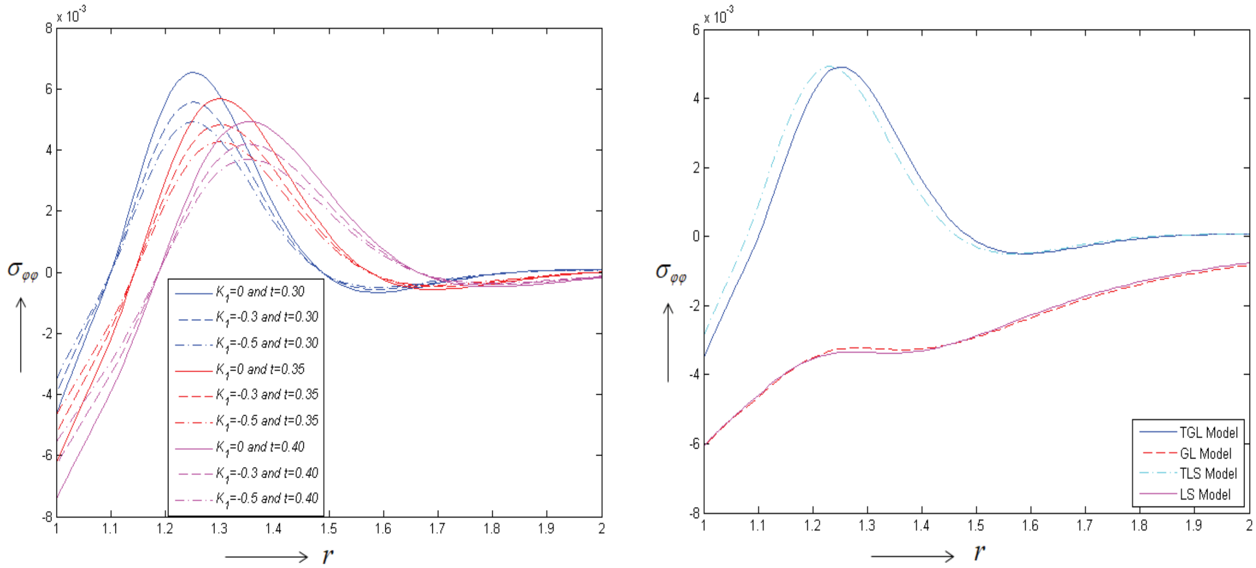

($\boldsymbol{a}$) ($\boldsymbol{b}$)

Figure 4.5: **($\boldsymbol{a}$).**Variation of $\sigma_{\varphi\varphi}$ vs. r under TGL model for different values of t and K_1, **($\boldsymbol{b}$).**Variation of $\sigma_{\varphi\varphi}$ vs. r for $K_1 = -0.5$ and $t = 0.3$ under different models

case of displacement distribution. However, difference between TGL model and TLS model or between GL model and LS model is not very prominent.

The variation of hoop stress, $\sigma_{\varphi\varphi}$ is shown in Figs. 4.5(a) and 4.5(b). Fig. 4.5(a) shows that the hoop stress is compressive in nature and the variation in $\sigma_{\varphi\varphi}$ is much prominent with respect to both time, t and temperature dependent material parameter, K_1. Further, it is observed that $\sigma_{\varphi\varphi}$ decreases with increase in time, t or with higher negative value of parameter, K_1. Here, we note that like the cases of other field variables, the difference in the nature of circumferential stress distribution under TGL and GL model is very much significant.